ELSEVIER

Journal of Organometallic Chemistry 573 (1999) 261–266

Journal of Organometallic Chemistry

Synthesis, chemical characterisation and molecular structure of $[Ag_3\{\mu_3\text{-}Fe(CO)_4\}(dppm)_3][NO_3]$ and $[Au_3\{\mu\text{-}Fe(CO)_4\}(dppm)_2][Cl]$[1]

Vincenzo G. Albano [a], Carlo Castellari [a], M. Carmela Iapalucci [b], Giuliano Longoni [b],*, Magda Monari [a], Alessandro Paselli [b], Stefano Zacchini [b]

[a] *Dipartimento di Chimica 'G. Ciamician', University of Bologna, via F. Selmi 2, 40126 Bologna, Italy*
[b] *Dipartimento di Chimica Fisica ed Inorganica, University of Bologna, viale Risorgimento 4, 40136 Bologna, Italy*

Received 16 April 1998

Abstract

The reaction of $Na_2[Fe(CO)_4] \cdot x$THF with $Ag_2(dppm)_2(NO_3)_2$ and $Au_2(dppm)_2Cl_2$, respectively affords the new $[Ag_3\{\mu_3\text{-}Fe(CO)_4\}(dppm)_3][NO_3]$ and $[Au_3\{\mu\text{-}Fe(CO)_4\}(dppm)_2][Cl]$ derivatives in high yields. These have been crystallised either from dichloromethane or THF by precipitation with hexane and an X-ray diffraction study has unambiguously shown that the $Fe(CO)_4$ unit is triply bridging in $[Ag_3\{\mu_3\text{-}Fe(CO)_4\}(dppm)_3]^+$ and doubly bridging in $[Au_3\{\mu\text{-}Fe(CO)_4\}(dppm)_2][Cl]$. The $[Ag_3\{\mu_3\text{-}Fe(CO)_4\}(dppm)_3]^+$ cation has also been obtained from degradation of $[Ag_{13}\{\mu_3\text{-}Fe(CO)_4\}_8]^{3-}$ with dppm. However, this preparation is less convenient owing to concomitant formation of iron carbonyl anions as side-products.

Keywords: Cluster; Iron; Silver; Gold; Carbonyl; Phosphine; Crystal structure

1. Introduction

A great number of neutral, anionic and cationic Au–Fe clusters, containing phosphine as ancillary ligand for gold, are known [1–3]. A few relevant examples with mono-dentate phosphine ligands are $Au_2Fe(CO)_4(PPh_3)_2$ [4,5], $Au_2Fe(CO)_4(PcHex_3)_2$ [6], $[Au_3Fe(CO)_4(PcHex_3)_3]^+$ [6], $[Au\{Fe_2(CO)_8\}PPh_3]^-$ [7], and $[Au\{Fe_3(CO)_{11}\}PPh_3]^-$ [8]. Bidentate phosphine ligands (P^P) such as bis-diphenylphosphine-methane (dppm) and bis-diphenylphosphine-ethane (dppe) has enabled the isolation of higher nuclearity species, e.g. $Au_4\{Fe(CO)_4\}_2(P^\wedge P)_2$ [9], $[Au_3\{Fe(CO)_4\}_2(P^\wedge P)]^-$ [10], $[Au_5\{Fe(CO)_4\}_2(P^\wedge P)_2]^+$ [10], $Au_2\{Fe_2(CO)_8\}$-(dppm) [11], and $[Au_2\{Fe_2(CO)_8\}_2(P^\wedge P)]^{2-}$ [11]. In all the above compounds the gold atoms are always coordinated by a single phosphorus atom. The length of the hydrocarbon spacer between the two phosphorus atoms of P^P seems to affect only the stability of a given species [11], and the geometry of the metal framework [9]. The corresponding chemistry of silver congeners has received much less attention [1,3]. To our knowledge the only relevant species are the neutral $Ag_6Fe_3(CO)_{12}$-$\{(PPh_2)_3CH\}$ [12] and $Ag_8\{Fe(CO)_4\}_4(dppm)_2$ compounds [13].

During the investigation of the synthesis of $Ag_8\{Fe(CO)_4\}_4(dppm)_2$ we have obtained spectroscopic evidence of the existence of other silver clusters stabilised concomitantly by $Fe(CO)_4$ and dppm ligands. We now report the synthesis and characterisation of the new $[Ag_3\{\mu_3\text{-}Fe(CO)_4\}(dppm)_3]^+$ cationic cluster; related attempts to synthesise the corresponding gold congener led to the isolation and characterisation of the $[Au_3\{\mu\text{-}Fe(CO)_4\}(dppm)_2][Cl]$ cluster, which differs

---

* Corresponding author. Fax: +39 51 6443690; e-mail: Longoni@ms.fci.unibo.it

[1] Dedicated to Professor Brian Johnson on the occasion of his 60th birthday in recognition of his outstanding contributions to organometallic and inorganic chemistry.

PII S0022-328X(98)00832-8

from the former in the stoichiometry, as well as in the stereochemistry of the $Fe(CO)_4$ moiety.

2. Results and discussion

2.1. Synthesis and molecular structure of $[Ag_3\{\mu_3\text{-}Fe(CO)_4\}(dppm)_3][NO_3]$

The $[Ag_3\{\mu_3\text{-}Fe(CO)_4\}(dppm)_3]^+$ cation has been selectively obtained by reaction of $[Ag_2(dppm)_2][NO_3]_2$ with $Na_2[Fe(CO)_4] \cdot x$THF in THF according to Eq. (1). The only side product detectable by IR during the reaction is $Ag_8\{Fe(CO)_4\}_4(dppm)_2$, which is generally present only in trace amounts.

$$2[Fe(CO)_4]^{2-} + 3[Ag_2(dppm)_2]^{2+} \rightarrow 2[Ag_3\{\mu_3\text{-}Fe(CO)_4\}(dppm)_3]^+ \quad (1)$$

The $[Ag_3\{\mu_3\text{-}Fe(CO)_4\}(dppm)_3][NO_3]$ salt has been isolated by filtration of the reaction solution, evaporation under vacuum of the THF and washing of the residue with water and toluene. Extraction in dichloromethane of the residue and precipitation by diffusion of hexane affords in $\approx 85\%$ yields yellow-orange crystals of $[Ag_3\{\mu_3\text{-}Fe(CO)_4\}(dppm)_3][NO_3]$ and $[Ag_3\{\mu_3\text{-}Fe(CO)_4\}(dppm)_3][NO_3] \cdot CH_2Cl_2 \cdot H_2O$ as two different crystalline forms. These crystals are soluble in most polar organic solvents and sparingly soluble or insoluble in water and non polar solvents such as hexane and toluene. In dichloromethane solution the $[Ag_3\{\mu_3\text{-}Fe(CO)_4\}(dppm)_3]^+$ cation shows infrared carbonyl absorptions at 1984s and 1849 vs cm^{-1}. The ^{31}P-NMR spectrum in d^6-acetone displays a very complex temperature-dependent pattern at δ 0–10 ppm (83% H_3PO_4 as reference), due to $^{31}P-^{107}Ag$, $^{31}P-^{109}Ag$ and $^{31}P-^{31}P$ couplings, which have previously been shown to extend over three bond distances in dinuclear and trinuclear carboxylate silver phosphine complexes [14]. In view of the chemical and spectroscopic complexity of these systems, investigations of ^{31}P-NMR spectra of $[Ag_3\{\mu_3\text{-}Fe(CO)_4\}(dppm)_3]^+$ and its related Ag–Fe and Au–Fe diphosphine clusters [10,13] are delayed until their chemistry will be clarified in some more detail.

An $Ag_3\{\mu_3\text{-}Fe(CO)_4\}$ moiety, as that found in the $[Ag_3\{\mu_3\text{-}Fe(CO)_4\}(dppm)_3]^+$ cation (see next), is the building motif of the $[Ag_{13}\{\mu_3\text{-}Fe(CO)_4\}_8]^{3-}$ anion [15]. Accordingly, the degradation with dppm of the latter affords the former; the degradation is complete only in the presence of excess dppm and gives rise to $[Fe(CO)_4]^{2-}$ and $[HFe(CO)_4]^-$ anions as additional carbonyl products. Their presence hampers the purification of the $[Ag_3\{\mu_3\text{-}Fe(CO)_4\}(dppm)_3]^+$ salts and, as a consequence, this alternative synthesis is less convenient than the above.

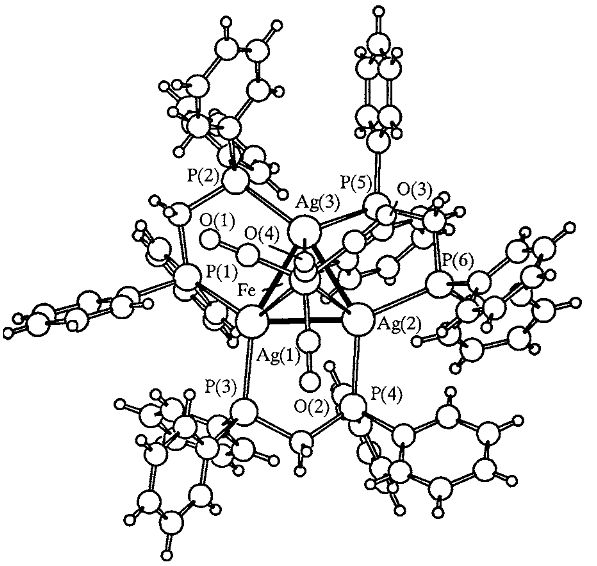

Fig. 1. Molecular structure of the $[Ag_3\{\mu_3\text{-}Fe(CO)_4\}(dppm)_3]^+$ cation present in $[Ag_3\{\mu_3\text{-}Fe(CO)_4\}(dppm)_3][NO_3] \cdot CH_2Cl_2 \cdot H_2O$.

The molecular structure of the $[Ag_3\{\mu_3\text{-}Fe(CO)_4\}(dppm)_3]^+$ cation is shown in Fig. 1, and relevant bond lengths and angles are reported in Table 1. The inner core of the cluster cation consists of an Ag_3 triangle with one face capped by an $Fe(CO)_4$ group adopting a C_{3v} geometry. Each edge of the Ag_3 triangle is bridged by dppm ligands whose phenyl groups are twisted in order to avoid steric hindrance. The metal framework can be better described as an Ag_3Fe tetrahedron. The cluster has a valence electron count of 60, as required by the EAN rule for the tetrahedron. The Ag–Ag distances are in a narrow range 2.932, 2.964, 3.004(1) Å and shorter than those found in $[Ag_3(\mu_3\text{-}Br)_2(dppm)_3]^+$ (average 3.303 Å) [16], and in $[Ag_3(\mu_3\text{-}Cl)_2(dppm)_3]^+$ (average 3.378 Å) [17]. The conformation of the three dppm ligands is influenced

Table 1
Selected bond lengths (Å) and angles (°) for $[Ag_3\{\mu_3\text{-}Fe(CO)_4\}(dppm)_3][NO_3] \cdot CH_2Cl_2 \cdot H_2O$

Ag(1)–Ag(2)	3.004(1)	Ag(3)–P(2)	2.507(3)
Ag(1)–Ag(3)	2.964(1)	Ag(3)–P(5)	2.520(3)
Ag(2)–Ag(3)	2.933(1)	Ag(2)–P(6)	2.553(3)
Ag(1)–Fe	2.794(2)	Ag(2)–P(4)	2.537(3)
Ag(2)–Fe	2.802(2)	Fe–C(1)	1.76(1)
Ag(3)–Fe	2.801(2)	C(1)–O(1)	1.17(1)
Ag(1)–P(1)	2.564(3)	Fe–C(2)	1.76(1)
Ag(1)–P(3)	2.543(3)	C(2)–O(2)	1.17(1)
Fe–C(3)	1.76(1)	Fe–C(4)	1.73(1)
C(3)–O(3)	1.17(1)	C(4)–O(4)	1.16(1)
P(1)–Ag(1)–P(3)	112.2(1)	Fe–Ag(3)–P(2)	120.39(8)
P(4)–Ag(2)–P(6)	112.0(1)	Fe–Ag(1)–P(1)	122.64(8)
Fe–Ag(1)–P(3)	122.54(8)	Fe–Ag(2)–P(4)	122.95(8)
P(2)–Ag(3)–P(5)	109.31(1)	Fe–Ag(2)–P(6)	119.14(8)
Fe–Ag(3)–P(5)	125.79(8)		

by the presence of the $Fe(CO)_4$ group on one face of the Ag_3 triangle. In fact the phenyl rings of the diphosphines are almost axial on the less hindered face and almost equatorial on the more hindered one on which the $Fe(CO)_4$ group is bonded. The three equatorial COs of the C_{3v} $Fe(CO)_4$ moiety are staggered with respect to the Ag_3 plane. The Ag–Fe interactions (2.794, 2.802, 2.803(2) Å) are equivalent and longer than the distances found in the neutral $[Ag_6\{\mu_3\text{-}Fe(CO)_4\}_3\{(Ph_2P)_3CH\}]$ [12], and $[Ag_{13}\{\mu_3\text{-}Fe(CO)_4\}_8]^{3-/4-}$ (average 2.69, 2.712 and 2.737 Å, respectively) [15,18]. All P atoms of the dppm ligands are displaced out of the Ag_3 plane away from the μ_3-$Fe(CO)_4$ group by 1.156, 1.097, 1.019, 0.639, 0.420, 0.380(3) Å, respectively.

The Ag_2P_2C rings are rather distorted and adopt envelope conformations with the CH_2 group of the dppm ligand at the flap position. The CH_2 groups point towards the face of the Ag_3 plane capped by $Fe(CO)_4$. The Ag–P interactions fall in the range 2.507–2.565(3) Å. The shortest contact between the anion NO_3^- and the cluster cation is with one hydrogen atom of the phenyl rings (O···H–C 2.56 Å) since the 'free' face of the Ag_3 plane is not accessible. The idealised molecular symmetry is C_{3v}, if the deformations induced by the packing forces are ignored.

2.2. Synthesis and molecular structure of $[Au_3\{\mu\text{-}Fe(CO)_4\}(dppm)_2][Cl]$

The corresponding reaction of $Au_2(dppm)_2Cl_2$ with $Na_2[Fe(CO)_4] \cdot x$THF has a more complicated course, and the nature of the final product greatly depends on the molar ratio between the reagents. IR monitoring shows that the reaction initially gives rise to the known $[Au_3\{\mu\text{-}Fe(CO)_4\}_2(dppm)]^-$ monoanion, which has previously been isolated from the related reaction between $Au_2(dppm)Cl_2$ and $Na_2[Fe(CO)_4] \cdot x$THF [10]. According to Eq. (2), the reaction is complete after addition of ca. 0.7 mol of $Au_2(dppm)_2Cl_2$ mol^{-1} of $Na_2[Fe(CO)_4] \cdot x$THF. Further addition of ca. 1.5 mol of $Au_2(dppm)_2Cl_2$ leads to the new $[Au_3\{\mu\text{-}Fe(CO)_4\}(dppm)_2][Cl]$ derivative (Eq. (3)), through the intermediate formation of a yet unknown species.

$$4[Fe(CO)_4]^{2-} + 3[Au_2(dppm)_2]^{2+} \rightarrow 2[Au_3\{\mu\text{-}Fe(CO)_4\}_2(dppm)]^- + 4\text{dppm} \qquad (2)$$

$$[Au_3\{\mu\text{-}Fe(CO)_4\}_2(dppm)]^- + 1.5Au_2(dppm)_2Cl_2 \rightarrow 2[Au_3\{\mu\text{-}Fe(CO)_4\}(dppm)_2][Cl] + Cl^- \qquad (3)$$

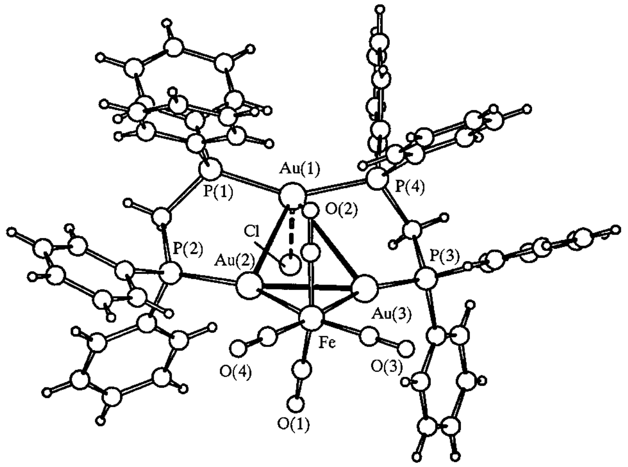

Fig. 2. Molecular structure of $[Au_3\{\mu\text{-}Fe(CO)_4\}(dppm)_2][Cl]$.

The $[Au_3\{\mu\text{-}Fe(CO)_4\}(dppm)_2][Cl]$ derivative has been crystallised by layering of hexane on its THF solution. The compound is soluble in dichloromethane, THF and acetone, sparingly soluble or insoluble in toluene, hexane and water. Its infrared spectrum is almost insensitive to the solvent. This consists of three distinct carbonyl absorptions which fall at 1996 s, 1924 s, 1896 ms cm^{-1} in THF, 1995 s, 1923 s and 1895 ms cm^{-1} in CH_3CN, and 1992 s, 1920 sh and 1890 s (broad) cm^{-1} in DMSO. The invariance of the absorption frequencies on changing the dielectric constant of the solvent suggests that the $[Au_3\{\mu\text{-}Fe(CO)_4\}(dppm)_2][Cl]$ derivative is dissociated in solution. The ^{31}P-NMR spectrum in d^6-acetone displays two multiplets centred at 33.8 and 39.1 ppm (83% H_3PO_4 as reference) in agreement with the different coordination sites of the two phosphorus atoms of dppm.

In view of the structural relationship between the $[Ag_3\{\mu_3\text{-}Fe(CO)_4\}(dppm)_3]^+$ cation and the $[Au_3\{\mu\text{-}Fe(CO)_4\}(dppm)_2][Cl]$ derivative (vide infra), it was of interest to verify the possible occurrence in solution of an equilibrium between the latter and a gold congener of the former in the presence of free dppm ligand; no trace of such equilibrium could be monitored by IR, even upon addition of a fivefold excess of phosphine.

The molecular structure of the $[Au_3\{\mu\text{-}Fe(CO)_4\}(dppm)_2][Cl]$ derivative is shown in Fig. 2 and relevant bond lengths and angles are reported in Table

Table 2
Selected bond lengths (Å) and angles (°) for $[Au_3\{\mu_3\text{-}Fe(CO)_4\}(dppm)_2][Cl]$

Au(1)–Au(2)	3.266(1)	Au(3)–P(3)	2.273(3)
Au(1)–Au(3)	3.556(1)	Fe–C(1)	1.79(1)
Au(2)–Au(3)	3.044(1)	Fe–C(2)	1.77(1)
Au(2)–Fe	2.538(1)	Fe–C(3)	1.76(1)
Au(3)–Fe	2.518(2)	Fe–C(4)	1.76(1)
Au(1)–Cl	2.805(3)	C(1)–O(1)	1.16(1)
Au(1)–P(1)	2.306(3)	C(2)–O(2)	1.14(1)
Au(1)–P(4)	2.306(3)	C(3)–O(3)	1.15(1)
Au(2)–P(2)	2.281(2)	C(4)–O(4)	1.16(1)
Fe–Au(3)–P(3)	164.84(7)	Cl–Au(1)–Au(2)	88.10(6)
Fe–Au(2)–P(2)	154.72(7)	Cl–Au(1)–Au(3)	85.77(7)
P(1)–Au(1)–P(4)	150.21(8)	C(1)–Fe–C(2)	149.7(5)

2. The cluster consists of an irregular Au_3 triangle in which one edge is bridged by an $Fe(CO)_4$ group adopting a C_{2v} geometry and the other two are spanned by the two dppm ligands. The Fe atom lies 0.97 Å above the Au_3 plane (dihedral angle between Au(1)–Au(2)–Au(3) and Au(2)–Au(3)–Fe planes 28.58(5)°). The Au–Au distances spanned by the diphosphine ligands are rather scattered (Au(1)–Au(2) 3.266, Au(1)–Au(3) 3.556(1) Å) and comparable with those found in the recently reported anion $[Au_3\{\mu\text{-}Fe(CO)_4\}_2(dppm)]^-$ [3.578(2) Å] [10]. The Au–Au bond spanned by an $Fe(CO)_4$ group is the shortest in both compounds being 3.044(1) Å in the case under study and 2.921(1) in the aforementioned anion. The longest Au–Au distances among those just cited are beyond the sum of the van der Waals radii of gold (3.4 Å) [19]. The loosening of the Au-Au interactions spanned by dppm ligands are not to be attributed to the need of a wider 'bite' angle for the dppm ligand since shorter Au-Au contacts have been reported, for example in the neutral $Au_2Fe_2(CO)_8(dppm)$ [11], and $Au_4\{Fe(CO)_4\}_2(dppm)_2$ (2.915 and 3.163(1) Å, respectively) [9]. A possible explanation is that the Au–Au vectors are elongated in order to widen the P(1)–Au(1)–P(4) angle as close to 180° as possible, in view of the preferred linear coordination of gold(I), and the small steric relevance of the weak Au–Cl (see later) and Au–Au contacts. Conversely the Au–Fe bonds (2.538 and 2.518(1) Å) are shorter than the corresponding values observed in $[Au_3\{\mu\text{-}Fe(CO)_4\}_2(dppm)]^-$ (range 2.545–2.576(1) Å, average 2.562).

The coordination of Au(I) in the solid state is completed by a chloride ion lying almost orthogonal to the Au_3 plane and opposite to the $Fe(CO)_4$ moiety. The orientation of the Au–Cl interaction is very probably dictated by steric factors. The Au(1)–Cl distance (2.805(3) Å) is similar to that reported for the dinuclear $[Au_2\{Ph_2PC(CH_2)_2PPh_2\}_2Cl]^+$ (2.807(3) Å) [20] and slightly weaker than those reported for in $[Au_2(dppm)_2Cl_2]$ (2.771(4) Å) [21], and $[Au\{Ph_2PC(CH_2)PPh_2\}Cl]_2$ (2.723(2) Å) [22]. Quite significantly the chloride ion is in close contact with the gold atom bearing the highest net charge, being Au(2) and Au(3) bonded to the negatively charged $Fe(CO)_4$ unit. We choose to describe the Au(1)–Cl interaction as primarily ionic because truly covalent Au–Cl bonds are much shorter, for instance values as short as 2.248(9) and 2.265(8) Å have recently been reported for the $[AuCl_2]^-$ anion [23].

The Au–P distances are normal and fall in the range 2.273–2.306(3) Å being the two longer interactions (2.306(1) Å) those involving Au(I). The molecular symmetry is approximately C_s.

3. Conclusion

Several anionic Ag–Fe carbonyl clusters are known [15,18,24]. The syntheses of $[Ag_3\{\mu_3\text{-}Fe(CO)_4\}(dppm)_3]^+$ and previously reported complementary results [12,13] point out that neutral and cationic Ag–Fe carbonyl clusters can be stabilised through the intervention of bi- and tri-dentate phosphines as ancillary ligands. Corresponding species with mono-dentate phosphines, or related anionic clusters involving phosphines as ancillary ligands, are yet unknown probably due to their instability. The cluster charge and the bonding behaviour of the phosphine are much less critical in the case of gold [4–11]. Among the so far reported Au–Fe derivatives, the $[Au_3\{Fe(CO)_4\}_2(P^\wedge P)]^-$ ($P^\wedge P$ = dppm, dppe) anion has a key role and displays a great versatility as reagent. So far its reaction with $Au_2(P^\wedge P)_xCl_2$ ($x = 1, 2$) enabled the syntheses of $Au_4\{Fe(CO)_4\}_2(P^\wedge P)_2$ [9,10], $[Au_5\{Fe(CO)_4\}_2(P^\wedge P)_2]^+$ [10], and $[Au_3\{Fe(CO)_4\}(dppm)_2][Cl]$, upon variation of the molar ratio between the reagents and/or the reaction solvent. Furthermore, as shown by its reactions with uncoordinated Cu^+ ions, which affords $Cu_2Au_6\{Fe(CO)_4\}_4(P^\wedge P)_2$ by further exploitation of the bonding capability of the $\mu\text{-}Fe(CO)_4$ moieties [25], yet other species can be foreseen.

4. Experimental

All reactions including sample manipulations were carried out using standard Schlenk techniques under nitrogen and in carefully dried solvents. The $Na_2[Fe(CO)_4]\cdot x$THF ($x \approx 2$) salt was prepared according to the literature [26]. Analyses of Fe, Ag and Au were performed by atomic absorption on a Pye–Unicam instrument. Infrared spectra were recorded on a Perkin Elmer 1605 interferometer using CaF_2 cells. ^1H- and ^{31}P-NMR spectra were recorded on a Varian Gemini 300 MHz instrument.

4.1. Synthesis of $[Ag_3\{\mu_3\text{-}Fe(CO)_4\}(dppm)_3][NO_3]$

Solid $Na_2[Fe(CO)_4]\cdot 2THF$ (0.51 g, 1.42 mmol) and $Ag_2(dppm)_2(NO_3)_2$ (2.36 g, 2.13 mmol) were mixed in a 100 ml flask under a nitrogen atmosphere. Anhydrous THF (40 ml) was added and the suspension was rapidly stirred for 6 h. After this period of time IR monitoring only showed the presence of the infrared absorptions of $[Ag_3\{\mu_3\text{-}Fe(CO)_4\}(dppm)_3]^+$. The suspension was filtered and the resulting orange solution was evaporated to dryness under vacuum. The residue was washed with water (20 ml) and toluene (20 ml). Extraction of the residue with dichloromethane (40 ml) and precipitation by diffusion of hexane (70 ml) gave 2.06 g of a mixture of [$Ag_3\{\mu_3$-$Fe(CO)_4\}(dppm)_3][NO_3]$ (predominant component) and [$Ag_3\{\mu_3$-$Fe(CO)_4\}(dppm)_3][NO_3] \cdot CH_2Cl_2 \cdot H_2O$ as yellow-orange crystals. The analysis of the mixture gave the following results: Found: Ag 18.41, Fe 3.18, C 55.04, H 3.80. Calcd for [$Ag_3\{\mu_3$-$Fe(CO)_4\}(dppm)_3][NO_3]$: Ag 19.0, Fe 3.27, C 55.59, H 3.87. ^{1}H-NMR (d^6-acetone, 25°C) at δ 3.55 (m, 2 H, CH_2) and 7.1–7.3 ppm (m, 10H, Ph).

4.2. Synthesis of [$Au_3\{\mu$-$Fe(CO)_4\}(dppm)_2][Cl]$

Solid $Na_2[Fe(CO)_4] \cdot 2THF$ (0.27 g, 0.75 mmol) and $Au_2(dppm)_2Cl_2$ (1.4 g, 1.13 mmol) were mixed in a 100 ml flask under a nitrogen atmosphere. Anhydrous THF (30 ml) was added and the suspension was rapidly stirred for six hours. The resulting orange-red suspension was evaporated to dryness under vacuum and the residue was washed with water (50 ml in portions) and toluene (20 ml). Extraction of the residue with THF (40 ml) and precipitation by diffusion of hexane (70 ml) gave 0.76 g of [$Au_3\{\mu$-$Fe(CO)_4\}(dppm)_2][Cl]$ as orange crystals. Anal. Found: Au 37.41, Fe 3.32, C 41.37, H 2.78; Calcd for of [$Au_3\{\mu$-$Fe(CO)_4\}(dppm)_2][Cl]$: Au 37.82, Fe 3.57, C 41.48, H 2.82. ^{1}H-NMR (d^6-acetone, 25°C) at δ 3.65 (m, 2 H, CH_2) and 7.4–7.8 ppm (m, 10H, Ph).

4.3. Crystal structures determination

Crystal data and details of the data collection for [$Ag_3\{\mu_3$-$Fe(CO)_4\}(dppm)_3][NO_3] \cdot CH_2Cl_2 \cdot H_2O$ and for [$Au_3\{\mu$-$Fe(CO)_4\}(dppm)_2][Cl]$ are given in Table 3. The diffraction experiments were carried out at r.t. on a fully automated Enraf–Nonius CAD-4 diffractometer using graphite-monochromated Mo–K_α radiation on crystals sealed in Lindeman glass capillaries. The unit cell parameters were determined by a least-squares fitting procedure using 25 reflections. Data were corrected for Lorentz and polarisation effects. No decay correction was necessary. An empirical absorption correction was applied by using the azimuthal scan method [27].

[$Ag_3\{\mu_3$-$Fe(CO)_4\}(dppm)_3][NO_3] \cdot CH_2Cl_2 \cdot H_2O$. The space group $P2_1/n$ was determined on the basis of systematic absences. The positions of the metal atoms were found by direct methods using the SHELXS 86 program [28] and all the non-hydrogen atoms located from Fourier-difference maps. One dichloromethane and one water molecule were also found in the asymmetric unit. The phenyl rings of the diphoshine ligands were refined as rigid hexagons (C–C 1.39, C–H 0.93 Å, C–C–C 120°) and all the hydrogen atoms of the dppm ligands added in calculated positions. The final refinement on F^2 proceeded by full-matrix least-squares calculations (SHELXL 93) [29] using anisotropic thermal parameters only for Ag, Fe, CO and NO_3^- because of the limited number of observed data. The methylene and the phenyl H atoms were assigned an isotropic thermal parameter 1.2 times U_{eq} of the carbon atoms to which they were attached. In the final Fourier-difference map the electron density was found in the range -0.54 and 0.86 e Å^{-3}.

Table 3
Crystal data and experimental details for [$Ag_3\{\mu_3$-$Fe(CO)_4\}(dppm)_3][NO_3] \cdot CH_2Cl_2 \cdot H_2O$ and [$Au_3\{\mu$-$Fe(CO)_4\}(dppm)_2][Cl]$

Formula	$C_{79}H_{66}Ag_3FeNO_7P_6 \cdot CH_2Cl_2 \cdot H_2O$	$C_{54}H_{44}Au_3ClFeO_4P_4$
M	1807.52	1562.97
Temperature (K)	293(2)	293(2)
Wavelength (Å)	0.71069	0.71069
Crystal symmetry	Monoclinic	Monoclinic
Space group	$P2_1/n$ (No. 14)	$P2_1/n$ (No. 14)
Unit cell dimensions		
a (Å)	13.427(2)	14.415(5)
b (Å)	25.800(9)	15.727(9)
c (Å)	22.61(1)	24.349(6)
β (°)	94.11(3)	103.79(2)
Cell volume (Å^3)	7811(5)	5631(4)
Z	4	4
D_{calc} (mg m^{-3})	1.537	1.937
μ (Mo–K_α) (mm^{-1})	1.169	8.662
$F(000)$	3640	2960
Crystal size (mm)	$0.25 \times 0.35 \times 0.37$	$0.25 \times 0.30 \times 0.32$
θ Limits (°)	2–20	2–20
Scan mode	ω	ω
Reflections collected	7227 ($+h$, $+k$, $\pm l$)	4605($\pm h$, $+k$, $+l$)
Unique observed reflections [$F_o > 4\sigma(F_o)$]	4500	3708
Goodness-of-fit on F^2	1.003	1.021
$R_1(F)^a$, $wR_2(F^2)^b$	0.0480, 0.1248	0.0249, 0.0654
Weighting scheme	$a = 0.0856$, $b = 34.389^b$	$a = 0.0483$, $b = 9.336^b$
Largest difference peak and hole (e Å^{-3})	0.789 and -0.538	0.541 and -0.567

[a] $R_1 = \Sigma\|F_o| - |F_c|/\Sigma|F_o|$.
[b] $wR_2 = [\Sigma w(F_o^2 - F_c^2)^2/\Sigma w(F_o^2)^2]^{1/2}$ where $w = 1/[\sigma^2(F_o^2) + (aP)^2 + bP]$ where $P = (F_o^2 + 2F_c^2)/3$.

Another data set had previously been collected for [$Ag_3\{\mu_3$-$Fe(CO)_4\}(dppm)_3][NO_3]$: $a = 12.70(1)$, $b = 14.354(7)$, $c = 22.37(1)$ Å, $\alpha = 94.89(4)$, $\beta = 99.95(5)$, $\gamma = 101.09(7)$°, triclinic, space group $P\bar{1}$, $V = 3910(5)$ Å^3, $Z = 2$, $R_1 = 0.0763$, $wR_2 = 0.1889$. Because of the better quality of the former data set and of the fact that the two crystals contained the same species crystallised with and without solvents, respectively only the more accurate molecular structure, determined in the monoclinic crystals, is reported here.

[$Au_3\{\mu$-$Fe(CO)_4\}(dppm)_2][Cl]$. The space group $P2_1/n$ was determined on the basis of systematic absences. The positions of the metal atoms were found by direct methods using the SHELXS 86 program [28] and all the non-hydrogen atoms located from Fourier-difference maps. The phenyl rings of the diphoshine ligands were treated as for $[Ag_3\{\mu_3\text{-}Fe(CO)_4\}(dppm)_3][NO_3] \cdot CH_2Cl_2 \cdot H_2O$. The final refinement on F^2 proceeded by full-matrix least-squares calculations (SHELXL 93) [29] using anisotropic thermal parameters for all the non hydrogen atoms.

A complete list of bond lengths and angles, and tables of hydrogen coordinates and anisotropic displacement parameters, have been deposited at the Cambridge Crystallographic Data Centre.

Acknowledgements

We wish to acknowledge financial support from the EEC, MURST and the University of Bologna (projects 'Sintesi, modelli e caratterizzazione per materiali funzionali' and 'Molecole e aggregati molecolari intelligenti')

References

[1] I.D. Salter, Adv. Organomet. Chem. 29 (1989) 249.
[2] K.P. Hall, D.M.P. Mingos, Prog. Inorg. Chem. 32 (1984) 237.
[3] C.E. Holloway, W.A. Nevin, M. Melnik, J. Coord. Chem. 31 (1994) 191.
[4] C.E. Coffey, J. Lewis, R.S. Nyholm, J. Chem. Soc. (1964) 1741.
[5] V.G. Albano, M. Monari, M.C. Iapalucci, G. Longoni, Inorg. Chim. Acta 213 (1993) 183.
[6] R.V. Parish, L.S. Moore, A.J.D. Dens, D.M.P. Mingos, D.J. Sherman, J. Chem. Soc. Dalton Trans. (1988) 781.
[7] O. Rossell, M. Seco, P.G. Jones, Inorg. Chem. 29 (1990) 348.
[8] O. Rossell, M. Seco, R. Reina, M. Font-Bardia, X. Solans, Organometallics 13 (1994) 2127.
[9] C.E. Briant, K.P. Hall, D.M.P. Mingos, J. Chem. Soc. Chem. Commun. (1983) 843.
[10] V.G. Albano, M.C. Iapalucci, G. Longoni, L. Manzi, M. Monari, Organometallics 16 (1997) 497.
[11] S. Alvarez, O. Rossell, M. Seco, J. Valls, M.A. Pellinghelli, A. Tiripicchio, Organometallics 10 (1991) 2309.
[12] C.E. Briant, R.G. Smith, D.M.P. Mingos, J. Chem. Soc. Chem. Commun. (1984) 586.
[13] V.G. Albano, M.C. Iapalucci, G. Longoni, M. Monari, A. Paselli, S. Zacchini, Organometallics, in press.
[14] A.F.M.J. Van Der Ploeg, G. Van Koten, Inorg. Chim. Acta 51 (1981) 225.
[15] V.G. Albano, F. Calderoni, M.C. Iapalucci, G. Longoni, M. Monari, P. Zanello, J. Cluster Sci. 6 (1995) 107.
[16] A.A.M. Aly, D. Neugebauer, O. Orama, U. Schubert, H. Schmidbaur, Angew. Chem. Int. Ed. Engl. 17 (1978) 125.
[17] D. Franzoni, G. Pelizzi, G. Predieri, P. Tarasconi, F. Vitali, C. Pelizzi, J. Chem. Soc. Dalton Trans. (1989) 247.
[18] V.G. Albano, L. Grossi, G. Longoni, M. Monari, S. Mulley, A. Sironi, J. Am. Chem. Soc. 114 (1992) 5708.
[19] A. Bondi, J. Phys. Chem. 68 (1964) 441.
[20] H. Schmidbaur, Th. Pollock, R. Herr, F.E. Wagner, R. Bau, J. Riede, G. Muller, Organometallics 5 (1986) 566.
[21] H. Schmidbaur, A. Wohllben, U. Schubert, A. Frank, G. Huttner, Chem. Ber. 110 (1977) 2751.
[22] H. Schmidbaur, R. Herr, G. Muller, J. Riede, Organometallics 4 (1985) 1208.
[23] D. Belli Dell'Amico, F. Calderazzo, N. Pasqualetti, R. Hübener, C. Maichle-Mössmer, J. Strähle, J. Chem. Soc. Dalton Trans. (1995) 3917.
[24] V.G. Albano, F. Azzaroni, M. C. Iapalucci, G. Longoni, M. Monari, S. Mulley, D.A. Proserpio, A. Sironi, Inorg. Chem. 33 (1994) 5320.
[25] V.G. Albano, M.C. Iapalucci, G. Longoni, M. Monari, M. Rauccio, S. Zacchini, work in progress
[26] J.P. Collman, R.G. Finke, J.N Cawse, J.I. Brauman, J. Am. Chem. Soc. 99 (1977) 2515.
[27] A.C.T. North, D.C. Philips, F.S. Mathews, Acta Crystallogr Sect A 24 (1968) 351.
[28] G.M. Sheldrick, SHELXS 86, Program for crystal structure solution, University of Gottingen, Gottingen, 1986.
[29] G.M. Sheldrick, SHELXL 93, Program for crystal structure refinement, University of Gottingen, Gottingen, 1993.